Removal of methylene blue from aqueous solution by activated carbon of *Vigna mungo L* and *Paspalum scrobiculatum* - Equilibrium, kinetics and thermodynamic studies

S. Valliammai, Y. Subbareddy, K. S. Nagaraja and B. Jeyaraj*

Department of Chemistry, Loyola Institute of Frontier Energy (LIFE), Loyola College, Chennai, TN, India

_____

ABSTRACT

The adsorption capacity of the activated carbons of Vigna mungo L (Black gram husk - ACBGH) and Paspalum scrobiculatum (Varagu millet Husk - ACVMH) were studied for the removal of Methylene blue (MB) from aqueous solutions. The surface area of the ACBGH and ACVMH was found to be 480.10 m^2/g and 397.33 m^2/g respectively. The adsorbents were also characterized by using Fourier Transform Infrared spectroscopy (FTIR), Scanning Electron Microscopy (SEM). Adsorption studies were performed to study the effects of contact time, initial concentration, temperature and pH. The data best fitted with the Langmuir model, with a maximum adsorption capacity of 198.40 mg g^{-1} and 166.30 mg g^{-1} for ACBGH and ACVMH respectively. The pseudo-second-order kinetics was the best for the adsorption of MB by the adsorbents. Thermodynamic studies showed that the adsorption was spontaneous, endothermic and entropy controlled. The results suggest that ACBGH and ACVMH can be used as a potential low-cost adsorbent for the MB dye removal from aqueous solution.

Keywords: Activated carbon, Methylene blue, Adsorption, Isotherms, Kinetics, Thermodynamics

_____

INTRODUCTION

Large amount of waste water is generated from industries such as dyestuffs, textile, paper and plastics. There are more than 100,000 commercially available dye and more than 7x 10^5 metric tons of dyes are produced worldwide annually [1] Colour is highly visualized in water and hence has to be removed before allowing it to enter into the water bodies. Colour prevents light penetration, inhibits photosynthetic activity, growth of living organism and also has a tendency to chelate metal ions which results in micro toxicity to fish and other organisms [2].It is estimated that about 2% of dyes that are produced are discharged directly in aqueous effluent during the manufacturing process and during the textile coloration process almost 10% of the dye loss occurs [3].

Many of the dyes are very poisonous when it is let into the nearby water bodies. It also causes serious hazard to living organisms under water. Among the various dyes used Methylene blue (MB) is the most commonly used dye for dyeing the natural fibers as cotton or silk. It can cause eye burns by direct contact and nausea, vomiting, profuse sweating, mental confusion and methemoglobinemia by ingestion [1]. Hence the treatment of effluent containing such dyes is compulsory.

For several decades various methods have been evolved in wastewater treatment such as electrochemical treatment methods, oxidation and ozonation [4]. Even though there are various methods adsorption has been proven as a most

_____

effective and reliable method for the removal of dye. Adsorption method of treatment is preferred for the less investment in terms of initial development cost, simple design, easy operations, free from generation of toxic substances and easy and safe recovery of the adsorbent as well as adsorbate materials [5]. Many low- cost adsorbents have been used for this purpose such as banana peels [6], rice straw [7], papaya seeds [8], orange peels [9], saw dust [10], wheat shells, and brans [11], but there is still a need for adsorbents which are cheap, easily available, and efficient.

Activated carbon has been found to be an effective adsorbent having high surface area and high adsorption capacity [12]. Activation methods involve physical activation such as carbonization of material and chemical activation such as using chemical activating agents. Many cheap, easily available agricultural and/or plant-based materials such as silk cotton hull, coconut tree sawdust, sago industry waste, banana pith, maize cob [13], rattan sawdust [14], jute fiber [15], pistachio shells [16], palm kernel shell [17], date pits [18], rice bran [19], coir pith [20], rice husk [21], mango seed kernel powder [22], rubber wood sawdust [23], plum kernels [24], rosewood sawdust [25], straw [26], coconut coir dust [27], palm fiber [28], pine cone [29], walnut shell, almond shell, hazelnut shell, apricot stones [30], coconut shells, groundnut shell, bamboo dust [31],deoiled soya [32], and wheat husk [33] have been used as a source of the production of activated carbon for the removal of textile dye effluents. Adsorption by activated carbon is an important way to clean up effluents and waste water, where it used to polish the influent before it is discharged into the environment [34].

Black Gram belongs to the family *Leguminoseae* bearing the botanical name as *Vigna mungo L.* It is one of the important pulse crops in India. It is reported that Black gram is originated in India and is the largest producer and consumer in the world. It is a rich protein food which contains about 26 percent protein, almost three times that of cereals. Black gram supplies a major share of protein requirement of vegetarian population of the country. Black gram originated in India, where it has been in cultivation from ancient times and is one of the most highly priced pulses of India and Pakistan. The coastal Andhra region in Andhra Pradesh is famous for black gram after paddy. The Guntur District ranks first in Andhra Pradesh for the production of black gram. Black gram has also been introduced to other tropical areas mainly by Indian immigrants.

Paspalum scrobiculatum, kodo millet, also known as cow grass, rice grass, ditch millet, Native Paspalum or Indian Crown Grass originates in tropical Africa, and it is estimated to have been domesticated in India 3000 years ago. Kodo millet is an annual grain that is grown in primarily in India, but also in the Philippines, Indonesia, Vietnam, Thailand, and in West Africa where it originates. It is grown as a minor crop in most of these areas, with the exception of the Deccan plateau in India where it is grown as a major food source. It is a very hardy crop that is drought tolerant and can survive on marginal soils where other crops may not survive, and can supply 450–900 kg of grain per hectare.

EXPERIMENTAL SECTION

2.1 Adsorbate.
Methylene blue (CI 52015) is a heterocyclic aromatic chemical compound with the molecular formula $C_{16}H_{18}N_3SCl$ and IUPAC name as 3, 7-bis (dimethylamino)-phenothiazin-5-ium chloride. The solution was prepared in doubly distilled water. All the test solutions were prepared by diluting the stock solution with double distilled water.

2.2 Preparation of adsorbents
Black gram husk and Millet Husk collected from the mills in Chennai, after removal of the pulses, were washed several times with water to remove any adhering substances and dried at room temperature. These were powdered by grinding in a mechanical blender and sieved. All the above collected materials were impregnated with orthophosphoric acid at $450^{o}C$ for 1hr in a muffle furnace. The carbonized materials were washed with water until neutral pH was obtained. It was dried at $110^{o}C$ overnight and grinded into powder. These activated carbons serve as the adsorbents namely ACBGH and ACVMH for Black gram husk and Millet Husk respectively.

2.3 Adsorption experiment
The experiment to observe the effect of important parameter like pH, adsorbent dose, contact time and temperature on the adsorptive removal of MB was conducted at 305±1 K. For each experimental run, 50 ml of MB solution of known concentration and a known amount of the adsorbent were taken in a 100 ml stoppered conical flask. This mixture was agitated in a temperature-controlled shaker and samples were centrifuged for 10 min for the suspended

_____

particles to settle down. After centrifugation clear supernatant samples were obtained and their residual dye concentration was analyzed for absorbance at 663 nm by using a UV Visible spectrophotometer.

2.4 Kinetic study of MB on various adsorbents.

Experiments to determine the adsorption equilibrium time on various activated carbons for MB were performed for a time interval ranging from 5 to 120 min. A known weight of the adsorbents were placed in 100 ml stoppered conical flask containing 50 ml of the dye solution at known concentrations (1.2×10^{-3} M, $1.4x^{-3}$ M, $1.8x^{-3}$ M) under constant Shaking. The experiments were made without pH correction. The adsorbents were separated from dye solution by centrifugation. The supernatant was collected and the absorbance was measured using a UV-Visible Spectrophotometer (Elico) at an absorbance wavelength of 663. The adsorption amount at time t, qt (mg/g), was calculated by:

$$\text{Amount Adsorbed } (q_t) = (C_0 - C_t) \times \frac{V}{m} \qquad (1)$$

where C_0 and C_t (mol/L) are the concentrations of the dye solution initially and at time t respectively. V (L) is the volume of dye solution and m (g) is the mass of the adsorbent used.

RESULTS AND DISCUSSION

3.1 Characterization of the ACBGH and ACVMH
3.1.1 FTIR analysis of ACBGH and ACVMH.

The band around 3606 cm^{-1} and 3780 cm^{-1} was observed for the black gram husk and millet husk samples (Fig.1), which was attributed to the O-H stretching vibration of the hydroxyl functional groups of alcohols and phenols. The peak at 1590 cm^{-1} and 1594 cm^{-1} in ACBGH and ACVMH corresponds to stretching vibration of COO–. The bands at 2921.50 cm^{-1} and 2850.80 cm^{-1} in black gram husk and millet husk samples, indicates the presence of an aliphatic C-H stretching also specifically the methylene group sp^3 stretching. The bands around 1164 cm^{-1} and 1169.96 cm^{-1} in black gram and millet husk has been assigned to C-O stretching in acids, alcohols, phenols, ethers and/or ester groups. It is the stretching frequencies of the phenolic and lactonic groups.
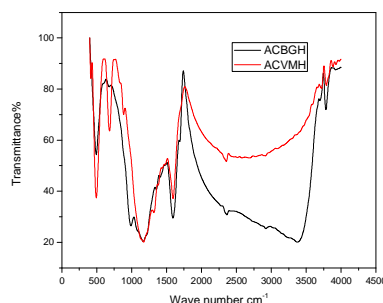

Fig.1 FTIR spectrum of ACGH and ACVMH

3.1.2. Scanning Electron Microscope Images.

Scanning electron microscopy (SEM) helps in finding the surface morphology and certain physical properties of the adsorbent. SEM of the adsorbent material was taken for ACBGH and ACVMH. The surface morphology of the activated carbon observed by SEM indicates that the activated carbon has different sizes of cavities. This might be due to the presence of mesoporous nature of activated carbon. These pores are large enough to allow the molecules of the dye to be adsorbed. From (Fig. 2a& b) it is clear that there is a good possibility for dyes to be trapped and adsorbed into these pores. The results showed that the major constituent was carbon (45.60%, 40.41%), along with some amount of hydrogen (2.15%, 1.76%) and nitrogen (1.94%, 0.75%).
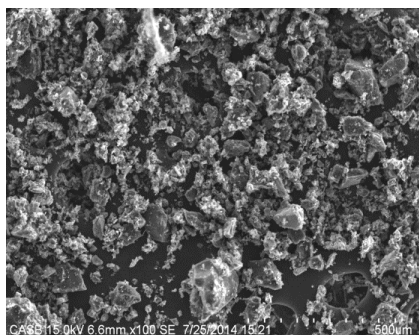
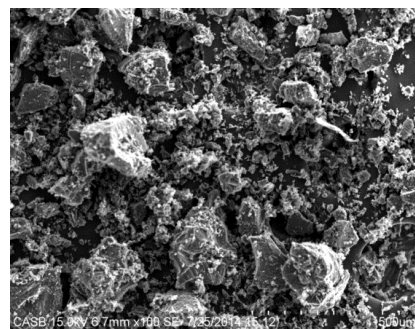_____

Fig.2a.SEM image of ACBGH   Fig.2b.SEM image of ACVMH

3.1.3. X-Ray Diffraction analysis

The X-ray diffraction pattern of the activated carbons exhibited two peaks at 2θ = 25.58, 26.45 and 41.48, 42.69 for black gram and millet husk respectively, which are attributed to (002) plane and (101) plane respectively (Fig.3) and which are similar to that of graphite [35] The crystallite size of ACBGH and ACVMH along L_c or L_a were determined by Scherer equation and found to be2.96 nm and 2.974 nm for L_c respectively. The interlayer spacing (d_{002}) was calculated using Bragg's equation [36].Typically, in a crystalline carbonaceous structure, such as graphite, the interlayer distance between two adjacent carbon sheets is 0.335 nm. In this study, the peaks at 2θ = 25.58, 26.45 corresponds to an interlayer distance of 0.348 nm and 0.335nm respectively for ACBGH and ACVMH, which is quite near to that of pure graphitic carbon [37].
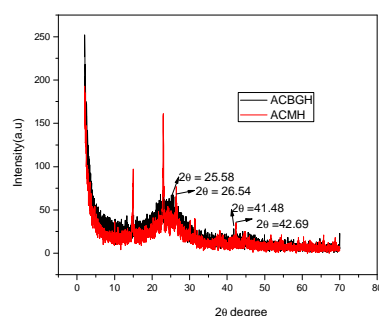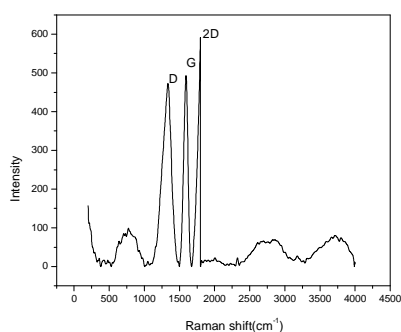

Fig.3. XRD pattern of NGC

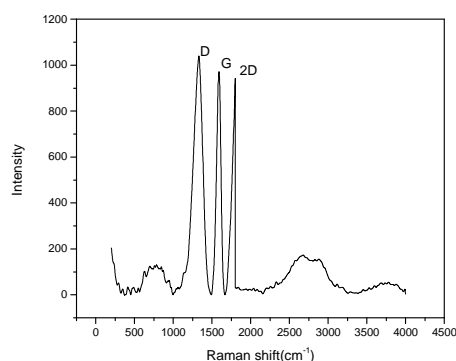**Fig.4a.Raman Spectrum of ACBGH**   **Fig.4b.Raman Spectrum of ACVMH**

3.1.4. Raman Spectroscopy

The graphitic nature of the adsorbents is further confirmed through Raman spectrum. The activated carbons exhibited two distinct peaks at about 1326 cm^{-1},1327 cm^{-1} (D- band) and 1598 cm^{-1}, 1594 cm^{-1} (G-band) respectively

_____

for ACBGH and ACVMH (Fig.4a&b). The G-band is related to the vibration of sp2 bonded carbon atoms in a two-dimensional hexagonal lattice, which often relates to the formation of ordered graphite layers. It is known that the relative intensity ratio between the D and G bands (ID/IG) reflects the degree of graphitization. Accordingly, the low ID/IG value indicates a high degree of graphitization [38].The ID/IG value of ACBGH and ACVMH is 0.8297, 0.8324 respectively, suggesting that the activated carbons has highly graphitic characteristic with high degree of graphite ordering.

3.1.5. BET analysis.
Pore characteristic of the activated carbon was determined byN2 adsorption. The activated carbons possessed type IV of IUPAC isotherm classification with H1 hysteresis. Due to the presence of hysteresis, the surface of the adsorbents confirms that of mesoporous in nature. The t-plot method was used to calculate the micropore volume and external surface area. Total pore volume was determined at $P/P_0 = 0.99$ for both the adsorbents. The pore characteristics of the activated carbons are given in Table 3. The average pore diameter of ACBGH and ACVMH was found to be 4.17nm and 6.75nm (Table1) which further confirms the presence of mesopores. The mesopore volume and micropore volume was found to be around 96.4% ,97.95%and 3.6% ,2.1% respectively of the total pore volume determined indicating that the adsorbents are mesoporous in nature.

Table 1: S_{BET} and pore structure of ACBGH and ACVMH

Adsorbent	S_{BET} (m^2/g)	S_{ext} (m^2/g)	S_{ext}/S_{BET} (%)	S_{mic} (m^2/g)	S_{mic}/S_{BET} (%)	V_{tot} (cm^3/g)	V_{mic} (cm^3/g)	V_{meso} (cm^3/g)	D_p (nm)
ACBGH	480.10	431.99	89.79	48.10	10.01	0.500	0.018	0.482	4.17
ACVMH	397.33	359.03	90.36	38.30	9.63	0.671	0.014	0.657	6.75

3.1.6. Zero point charge of the adsorbents
The point of zero charge of ACBGH and ACVMH was determined by solid addition method. In this method 0.1M KCl solution was taken in ten bottles maintained with pH in the range of 1-10 and 0.14g of ACBGH and 0.2g of ACVMH was added to each bottles .These solutions were shaken for 24h at room temperature and the final pH was measured. The difference between the initial and final pH was measured and the point where $\Delta pH = 0$ was taken as the point of zero charge. At pH<pHzpc, the surface has a net positive charge and at pH > pHzpc, it is negative. The pHzpc of ACBGH was found to be 2.0 and that of ACVMH was 2.1. The previous study of adsorption of Methylene blue onto sunflower oil cake activated carbon have found that the zero point of charge (pHzpc) for the activated carbon lies between pH 2.5 and 5.5 [39].

3.2. Effect of the amount of adsorbents
The study of the effect of amount of the adsorbents was carried out to observe the minimum possible amount, which shows maximum adsorption. Effect of the amount of adsorbents was carried out by selecting an adsorbent range of 0.04–0.32 g for black gram husk and Varagu millet husk with a dye concentration of 1.8 x 10^{-3}M concentration. A graphical representation (Fig.5) indicates that an increase in the amount of the adsorbent leads to an increase in the removal of the dye for both the system. The greater percentage adsorption at high adsorbent dosage is due to availability of more active sites of the adsorbents for the adsorption. An amount of 0.14 g and 0.2g was chosen as optimum amount for ACBGH and ACVMH respectively for the batch study of the adsorption process.
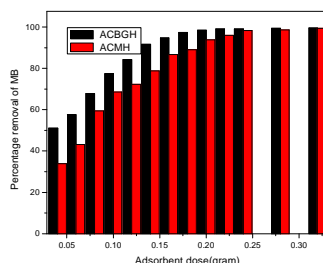

Fig.5. Effect of adsorbent dose for the adsorption MB onto ACBGH and ACVMH

3.3. Effect of concentration at varying temperatures.
Adsorption experiments for the dye MB were carried out by varying the concentration from 0.4 x10^{-3} to 2.6 x 10^{-3}M with an adsorbent dosage of 0.14 g and 0.2g of ACBGH and ACVMH respectively at 305K, 315K and 325K.The

_____

experimental results show that an increase in the concentration led to an increase in the amount of the dye adsorbed(Fig.6a and b) It is observed that the amount adsorbed increases from1.422 $x10^4$ mol/g to 7.2011 $x10^4$mol/g for black gram husk and from 0.9972 $x10^4$ mol/g to 5.7342 $x10^4$ mol/g for Varagu millet husk. For further studies, an optimum concentration of $1.8x10^{-3}$M of the dye solution was considered.
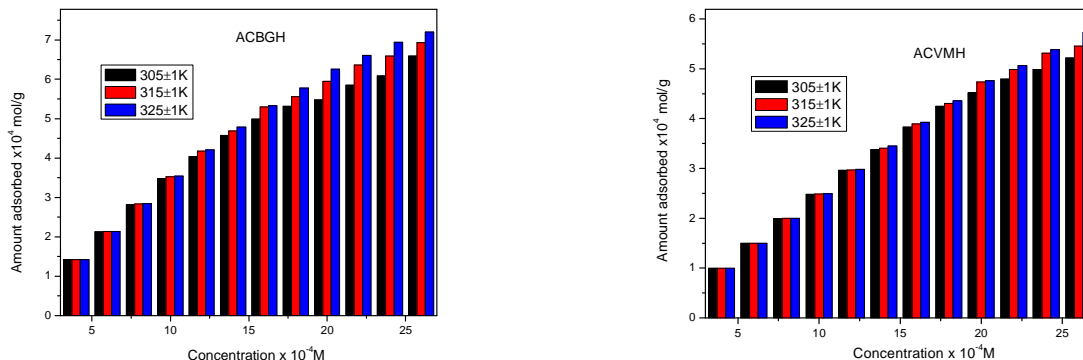

Fig.6a.Effect of concentration for the adsorption MB onto ACBGH at different temperatures
Fig.6b.Effect of concentration for the adsorption MB onto ACMVH at different temperatures

3.4. Effect of pH
As the pH affects the adsorption it is necessary to determine the adsorption behavior of the dye. The study of pH was carried out at predetermined experimental conditions taking initial dye concentration as $1.8x~10^{-3}$M. A pH range of 2 to 12 was selected for the adsorption of MB on ACBGH and ACVMH. Increase in the adsorption occurred, in the case of both adsorbent materials with the increase in pH from 2 to 12(Fig.7). Greater percentage adsorption is due to the electrostatic attraction between the negatively charged sites of the adsorbents and the positively charged dye molecules. This can be explained by considering the pHzpc of the adsorbents. The pHzpc of ACBGH and ACVMH was found to be 1.9 and 2.0 respectively. As pH of the system decreased below the pHzpc of the adsorbents, the number of negatively charged adsorbent sites decreased and the positively charged surface sites increased, which did not favour the adsorption of cationic dyes due to electrostatic repulsion. At higher pH, negatively charged adsorbent sites increased, which enhances the adsorption of positively charged dye cations through electrostatic forces of attraction [40]
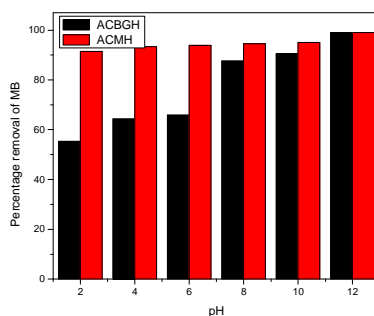

Fig.7 Effect of pH on ACBGH and ACVMH

3.5. Effect of contact time
Contact time plays a vital role in the adsorption studies as it suggests that necessary required time of contact for deriving maximum adsorption of the dye at the adsorbent surface. The amount of the dye adsorbed at definite intervals of time at ranging from 5 to 120 min was monitored for a fixed amount of the adsorbents (0.14 g of ACBGH and 0.2g of ACVMH) at a particular concentration. Experiments were carried out at a time interval ranging from 5 to 120 min for various concentrations of the dye solution as $1.2 x 10^{-3}$M, $1.4 x 10^{-3}$M and $1.8 x 10^{-3}$M. Fig.8a and b indicates that with the increase in time the adsorption rate of the dye over both adsorbents increases and almost120 min of time was required to bring complete saturation of the active sites of both adsorbents.
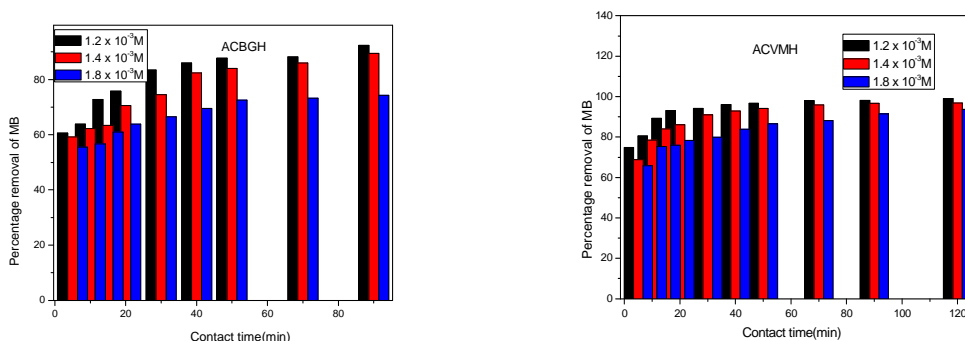
_____

Fig.8a. Effect of contact time for the adsorption of MB onto ACBGH
Fig.8b. Effect of contact time for the adsorption of MB onto ACVMH

3.6. Adsorption isotherm.

The equilibrium relationships between adsorbent and adsorbate are best explained by sorption isotherms. The present investigation deals with the applicability of Langmuir, Freundlich and D–R adsorption isothermal models to the experimental data. The thermodynamic parameters were calculated from the effect of temperature on the MB adsorption on the various activated carbons by using the Langmuir adsorption isotherms at different temperatures of 305K, 315K and 325K.

3.6.1. Freundlich isotherm

The Freundlich isotherm is a result of the assumption that the adsorption occurs on a heterogeneous surface and non-uniform distribution of the heat of adsorption over the adsorbent surface takes place. The Freundlich model was applied to calculate the adsorption data of MB, as per the given relation:

$$\log(q_e) = \log(K_f) + \frac{1}{n}\log(C_e) \tag{6}$$

K_f (mol/g) and n are the Freundlich constants, indicating adsorption capacity and adsorption intensity respectively. The graphical presentations for the Freundlich isotherm for the two adsorbents along with their R^2 values are given in Figs. 9a and b
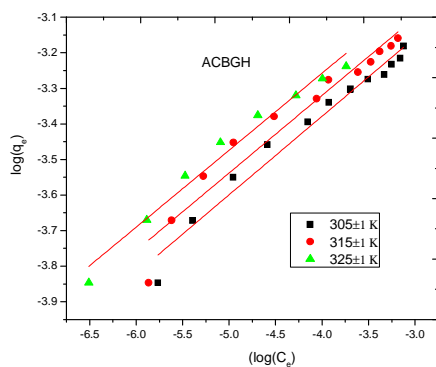

Fig. 9.a Freundlich Isotherm of ACBGH   **Fig.9b. Freundlich Isotherm of ACVMH**
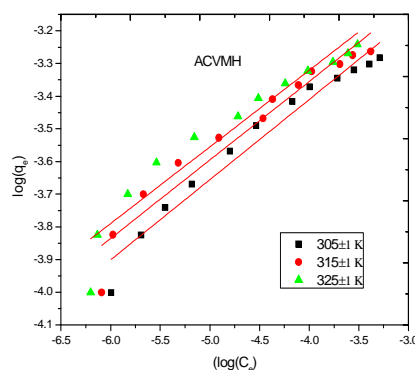
3.6.2. Langmuir isotherm

The Langmuir isotherm proposes that the coverage of adsorbate molecules on a solid surface occurs in a monolayer. It is assumed that once the adsorbent site is covered with the dye molecules no further adsorption occurs at that site. It also suggests that all the adsorption sites are of equivalent energy. Langmuir equation is stated as

$$\frac{C_e}{q_e} = \frac{1}{Q_m K_L} + \frac{1}{Q_m} C_e \tag{4}$$

601

_____

where, q_e(mol/g) and C_e(mol/L) are the amount of dye adsorbed per unit weight of adsorbent and the concentration of the dye solution at equilibrium respectively. The constant Q_m(mol/g) is the adsorption capacity and K_L (L/mol) is the Langmuir equilibrium constant. Figs. 10a and b show plots obtained for 1/qe against 1/Ce, at each temperature with the help of which Langmuir constants can be calculated (Table 2).
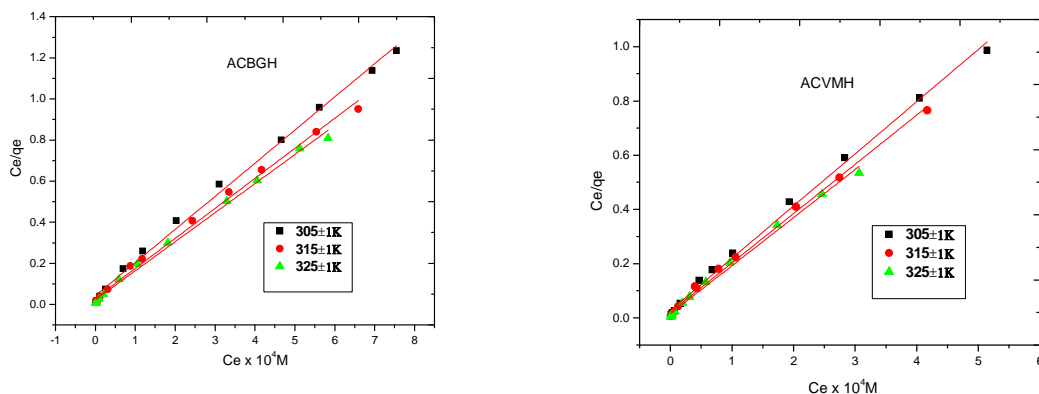

Fig.10.a Langmuir Isotherm plot of ACBGH   Fig.10 .b Langmuir Isotherm plot of ACVMH

On comparing the regression coefficients obtained for Freundlich and Langmuir it can be very well predicted that the Langmuir isotherm is more favoured by the adsorption process. The data presented above clearly show that Langmuir adsorption isotherm graphs are better fit than Freundlich adsorption isotherm graphs. The adsorption capacities of black gram husk and millet husk were found to be 198.40 and166.29mg/g respectively. The favourability of the adsorption process was also determined by calculating a dimensionless separation constant R_L by using the equation.

$$R_L = \frac{1}{1 + K_L C_0} \tag{5}$$

where C_0 is the initial dye concentration (mol/L) and K_L (L/mol)is Langmuir equilibrium constant. The value of R_L indicates the type of adsorption isotherm to be unfavorable ($R_L > 1$), linear ($R_L = 1$), favorable ($0 < R_L < 1$) or irreversible ($R_L = 0$).

3.6.3. Dubinin-Radushkevich (D-R) adsorption isotherm
Radushkevich adsorption isotherm was used to describe the adsorption on both homogeneous and heterogeneous surfaces. It is used to distinguish the adsorption taking place by physical or chemical processes. The linear form of the isotherm can be expressed as follows

$$\ln(q_e) = \ln(Q_m) - K\varepsilon^2 \tag{7}$$

where K is constant related to the adsorption constant (mol^2/kJ^2), and ε is the Polanyi potential that can be calculated from the equation.

$$\varepsilon = RT \ln\left(1 + \frac{1}{C_e}\right) \tag{8}$$

where R is the Universal gas constant (8.314 $Jmol^{-1}K^{-1}$), T is the temperature (K) and C_e is the concentration at equilibrium. Fig .11a and b shows the plot of ln (q_e) vs ε^2 of the experimental data for the adsorption of MB onto ACBGH and ACVMH. The slope gives K and from the intercept the adsorption capacity Q_m can be calculated.

The mean energy of sorption, *E* (kJ/mol), is calculated by the following equation.

$$E = \frac{1}{\sqrt{(2K)}} \tag{9}$$

_____

The mean sorption energy (E) calculated from D-R isotherm provides important information about the physical and chemical nature of the adsorption process. The mean energy of adsorption (E) in the range 15.35 to18.16 kJ/mol for MB indicates the involvement of chemisorption in the process.
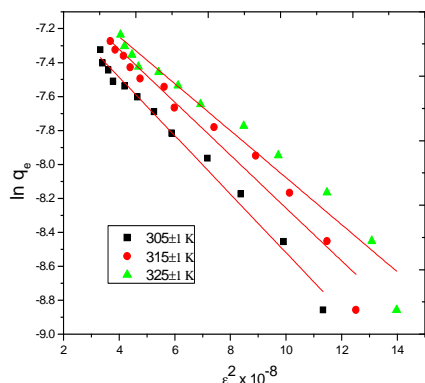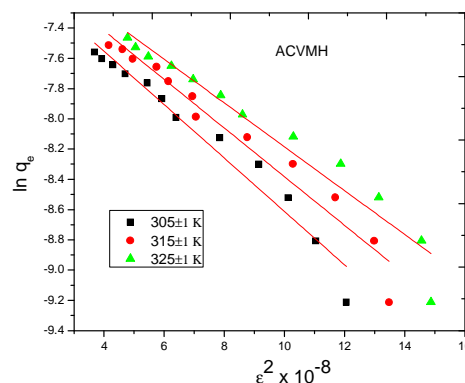

Fig.11.aD-R isotherm plot of ACBGH   **Fig. 11.b. D-R isotherm plots of ACVMH**

The graphs obtained in Langmuir plots further help in the determination of thermodynamic parameters. The thermodynamic parameters such as Gibbs free energy change ($\Delta G°$), enthalpy change ($\Delta H°$) and entropy change ($\Delta S°$) were calculated using the following relations. The thermodynamic parameters are calculated by using the well known equations.

Table 2: Adsorption isotherm parameters for the adsorption of MB onto ACBGH and ACVMH

	Temperature					
	305±1K	315±1K	325±1K	305±1K	315±1K	325±1K
	ACBGH			**ACVMH**		
Langmuir isotherm						
Q_m(mol/g)	6.203×10^{-4}	6.848×10^{-4}	7.074×10^{-4}	5.199×10^{-4}	5.506×10^{-4}	5.642×10^{-4}
K_L(l/mol)	3.781×10^{-4}	4.954×10^{-4}	6.254×10^{-4}	6.847×10^{-4}	8.414×10^{-4}	11.470×10^{-4}
R^2	0.99	0.99	0.99	0.99	0.99	0.99
R_L	0.062	0.048	0.038	0.035	0.028	0.021
Freundlich isotherm						
K_f(mol/g)	3.201×10^{-3}	3.573×10^{-3}	4.061×10^{-3}	3.725×10^{-3}	4.032×10^{-3}	4.146×10^{-3}
$1/n$	0.220	0.218	0.216	0.245	0.240	0.2345
n	4.525	4.582	4.618	4.075	4.163	4.263
R^2	0.96	0.93	0.97	0.95	0.93	0.92
Dubinin – Radushkevich isotherm						
Q_m (mol/g)	1.116×10^{-3}	1.232×10^{-3}	1.251×10^{-3}	1.061×10^{-3}	1.142×10^{-3}	1.186×10^{-3}
K (mol²/KJ²)	1.721×10^{-9}	1.558×10^{-9}	1.384×10^{-9}	1.763×10^{-9}	1.607×10^{-9}	1.448×10^{-9}
E (kJ/mol)	17.04	17.91	19.00	16.83	17.63	18.57
R^2	0.98	0.96	0.96	0.95	0.95	0.94

$$\Delta G^0 = -RT \ln K_L \tag{13}$$

$$\Delta H^0 = -R \frac{T_2 T_1}{T_2 - T_1} \ln \frac{K_{L2}}{K_{L1}} \tag{14}$$

$$\Delta S^0 = \frac{\Delta H^0 - \Delta G^0}{T} \tag{15}$$

The negative values of ΔG^0 (-26.72 to -29.84kJ/mol) and (-28.23 to -31.47kJ/mol) confirm the feasibility and spontaneous nature of the adsorption process. ΔH^0 (19.82kJ/mol and 26.36 kJ/mol) and ΔS^0 (152.63 J/molK and179.01 J/molK) are calculated and given respectively for ACBGH and ACVMH. The feasibility of the adsorption process is proved from the negative values of free energy. The positive nature of the enthalpy change and the entropy change confirms the endothermic nature of the process and affinity of the adsorbent towards adsorbate, respectively. The positive ΔS^0 value reflects that the adsorption mechanism is an entropy controlled process.

_____

3.7. Rate constant study
3.7.1. Lagergrens first-order kinetics

In order to determine the order of the ongoing adsorption process and also to evaluate the specific rate constants Lagergrens first-order rate equation was employed for both systems.

$$\log(q_e - q_t) = \log q_e - \frac{k_1}{2.303}t \qquad (10)$$

where q_e and q_t (mol/g) are the amounts adsorbed at equilibrium and at a time t and k_1 is the rate constant of the pseudo first order adsorption and presented in Figs 12a and b
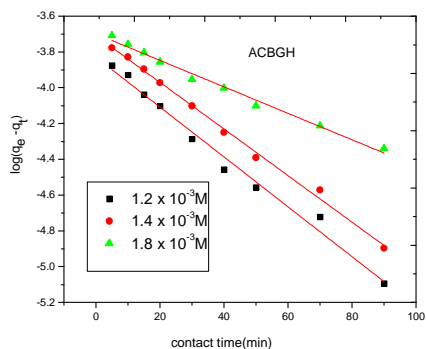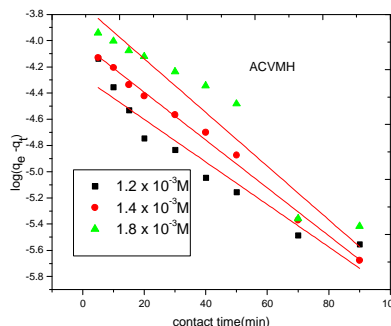

Fig.12a. Pseudo first order of ACBGH   **Fig.12.b. Pseudo first order of ACVMH**

3.7.2. Pseudo-second-order kinetics.

A second-order rate equation was also applied to ACBGH-MB and ACVMH–MB systems. The second-order rate expression is represented as

$$\frac{t}{q_t} = \frac{1}{k_2 q_e^2} + \frac{1}{q_e}t \qquad (11)$$

k_2 is the rate constant of the pseudo second order adsorption (g mol^{-1}min^{-1}).

The values of the various parameters (q_e, k_1 and k_2) were calculated by using the intercept and the slope obtained from the plots and tabulated in Table 3. Figs. 13a and b shows the plot of second order (t/q$_t$vs t) kinetic model.
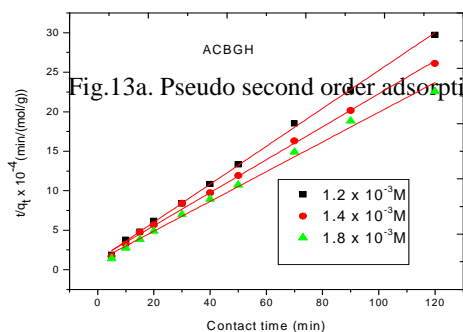

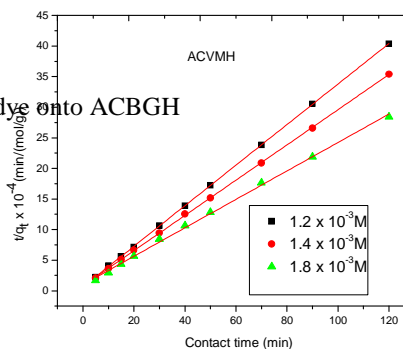Fig.13a. Pseudo second order adsorption of MB dye onto ACBGH

Fig.13b. Pseudo second order adsorption of MB dye onto ACMVH
Fig.13b. Pseudo second order adsorption of MB dye onto ACMVH

_____

R^2 values obtained for second-order kinetics are equal to unity, which is greater than that of first-order kinetics at all temperatures. This suggests that the second-order kinetic model is a perfect fit for the ACBGH-MB and ACVMH–MB systems.

Table 3: Adsorption kinetic parameters for the adsorption of MB by ACBGH and ACVMH

Adsorbate conc	Pseudo-first-order				Pseudo-second order		
	$q_e(exp)$ (mol/g)	k_1 (1/min)	$q_e(calc)$ (mol/g)	R^2	k_2 (g/mol min)	$q_e(calc)$ (mol/g)	R^2
ACBGH							
1.2×10^{-3}	4.035×10^{-4}	0.017	1.485×10^{-4}	0.985	0.474×10^3	4.165×10^{-4}	0.999
1.4×10^{-3}	4.595×10^{-4}	0.030	1.954×10^{-4}	0.995	0.313×10^3	4.789×10^{-4}	0.999
1.8×10^{-3}	5.317×10^{-4}	0.032	2.002×10^{-4}	0.987	0.250×10^3	5.313×10^{-4}	0.999
ACVMH							
1.2×10^{-3}	2.971×10^{-4}	0.037	0.529×10^{-4}	0.916	1.699×10^3	3.016×10^{-4}	0.999
1.4×10^{-3}	3.387×10^{-4}	0.042	0.937×10^{-4}	0.992	1.050×10^3	3.470×10^{-4}	0.999
1.8×10^{-3}	4.217×10^{-4}	0.047	1.868×10^{-4}	0.839	0.543×10^3	4.301×10^{-4}	0.999

3.8. Desorption studies
The percentage of desorption by water, HCl and NaOH are 2.87% and 0.98 respectively. When acetic acid, ethanol and acetone were used, it led to the desorption of 43.8%, 45.53% and 54.29% respectively. The maximum desorption occurred with acetone as the desorbing medium. The maximum desorption occurred with acetone. This further confirms that the process of adsorption is mainly chemical adsorption.

3.9. Testing of real effluent
To evaluate the efficiency of the prepared adsorbents towards the removal of the dyes, the real effluent collected from a textile industry was used. The adsorption of the dyes were performed with 50ml 0f the real effluent, with 0.4g and 0.5g of ACBGH and ACVMH respectively and allowed for shaking for 120minutes. The solution after filtration was subjected to physical and chemical examinations and the results are tabulated (Table.4).

Table.4 Physical and chemical examinations of the real Effluent

Physical Examination			
	Thirupur Effluent	ACBGH	ACVMH
Turbidity NT Units	36	16.9	15.2
Total dissolved solids mg/L	7170	5299	4914
Electrical conductivity Micro mho/cm	10243	7570	7020
Chemical Examination			
pH	8.22	6.966	.83
Total alkalinity	1840	456	408
Total Hardness	3200	476	508
Calcium as Ca mg/L	760	133	126
Magnesium as Mg mg/L	312	30	22
Sodium as Na mg/L	900	1405	1270
Potassium as K mg/L	160	45	35
Iron as Fe mg/L	0.82	0.70	0.63
Manganese as Mn mg/L	0	0	0
COD- mg/L	6060	281	277
BOD- mg/L	1800	100	90

CONCLUSION

From the above obtained values it is clear that ACBGH and ACVMH can be used in the removal of Methylene blue from the aqueous solution. The percentage of dye removed increased with increasing adsorbent dose, temperature and time, and decreased with increase in concentration. The isotherm study indicates that equilibrium data best fitted the Langmuir isotherm. The adsorption kinetic process was described by a pseudo-second-order rate model very well. The positive nature of the enthalpy change and the entropy change confirms the endothermic nature of the process and affinity of the adsorbent towards adsorbate, respectively. The positive ΔS^0 value reflects that the adsorption mechanism is an entropy controlled process. The tested results of the real effluent showed a decrease in the turbidity, Total dissolved solids and the BOD and the COD values. This concludes that the ACBGH and ACVMH is an efficient adsorbent for the removal of all the dyes.

_____

REFERENCES

[1] KAGGusmao; LVAGurgel; TMSMelo; LFGil; *Dyes Pigm*., **2012**, 92(3) , 967-974.

[2] MH Gad Hamdi; Ashraf AEl-Sayed; *J.Hazard Mater.,* **2009,** 168(2-3), 1070-1081.

[3] AMittal; JMittal; AMalviya; DKaur; VKGupta; *J. Colloid Interface Sci.,* **2010,** 343(2), 518-527

[4] AMittal; JMittal; AMalviya; VKGupta; *J. Colloid Interface Sci.,* **2009,** 340(1), 16-26.

[5] GCrini; *Bioresour Technol* ., **2006,** 97(9), 1061-1085.

[6] M Achak; A Hafidi; N Ouazzani; S Sayadi; L Mandi; *J Hazard Mater.,* **2009,** 166, 117–125.

[7] CG Rocha; DAM Zaia; RVS Alfaya; AAS Alfaya; *J. Hazard Mater.,* **2009,** 166(1), 383–388.

[8] BH Hameed; *J Hazard Mater.,* **2009,** 162(1), 939–944

[9] M Arami; NY Limaee; NM Mahmoodi; NS Tabrizi; *J. Colloid Interface Sci*., **2005,** 288(2), 371–376.

[10] FA Batzias; DK Sidiras; *Bioresour Technol* ., **2007,** 98(6), 1208–1217.

[11] A Mittal ; J Mittal ; A Malviya ; D Kaur ; VK Gupta; *J. Colloid Interface Sci*., **2010,** 343(2), 463–473.

[12] AMittal; JMittal; AMalviya; VKGupta; *J. Colloid Interface Sci*., **2010,** 344(2), 497-507.

[13] K Kadirvelu; M Kavipriya; C Karthika; M Radhika; N Vennilamani; S Pattabhi; *Bioresour Technol*., **2003**, 87(1),129–132.

[14] B H Hameed; A L Ahmad; K N A Latiff; *Dyes and Pigments.,* **2007**, 75,143–149.

[15] S Senthilkumaar; P R Varadarajan; K Porkodi; C V Subbhuraam; *J. Colloid Interface Sci.,***2005 ,** 284(1), 78–82.

[16] A A Attia; B S Girgis; S Khedr; *Journal of Chemical Technology and Biotechnology.,* **2003,** 78(6), 611–619.

[17] A Jumasiah; T G Chuah; J Gimbon; T S Y Choong; I Azni; *Desalination.,***2005**, 186(1-3) , 57–64.

[18] F Banat; S Al-Asheh; L Makhadmeh; *Adsorption Science and Technology.,* **2003,** 21 (6), 597–606.

[19] M Sankar; G Sekaran; S Sadulla; T Ramasami; *Journal of Chemical Technology and Biotechnology***., 1999,** 74(4) , 337–344.

[20] D Kavitha ; C Namasivayam; *Bioresource Technology.,* **2007**,98(1), 4–21.

[21] V K Gupta; A Mittal; R Jain; M Mathur; S Sikarwar; *J. Colloid Interface Sci.,***2006,** 303(1), 80–86.

[22]K Vasanth ;A Kumaran; *Biochemical Engineering Journal.,* **2005,** 27(1) ,83–93.

[23] B G P Kumar; L R Miranda; M Velan; *Journal of Hazardous Materials.,***2005**, 126(1-3), 63–70.

[24] R S Juang; F C Wu; R L Tseng; *Journal of Colloid and Interface Science*., **2000**, 227(2), 437–444.

[25] V K Garg; M Amita; R Kumar; R Gupta; *Dyes and Pigments*., **2004 ,** 63(3), 243–250.

[26] N Kannan; M Meenakshisundaram; *Water; Air; and Soil Pollution*., **2002,** 138(1-4), 289–305.

[27] J S Macedo; N B Júnior; L E Almeida; *J. Colloid Interface Sci.,***2006,** 298(2) , 515–522.

[28] I A W Tan; B H Hameed; W A L Ahmad; *Chemical Engineering Journal.,* **2007,** 127 (1-3) , 111–119.

[29] Ü Geçgel; K Sezer; H Kolancılar; *Asian Journal of Chemistry.,* **2010**,22(5), 3936–3942.

[30] A Aygün; S Yenisoy-Karakaş; I Duman; *Microporous and Mesoporous Materials.,* 2003, 66(2-3), 189–195.

[31] N Kannan ;M M Sundaram; *Dyes and Pigments.,* **2001,** 51(1) , 25–40.

[32] V K Gupta; A Mittal; V Gajbe; and J Mittal; *J. Colloid Interface Sci*., **2008**, 319(1), 30–39.

[33] V K Gupta; R Jain; and S Varshney; *Journal of Hazardous Mater.,* **2007,** 142(1-2), 443–448.

[34] MAMSalleh; DKMahmoud; WAWAKarim ; AIdris., *Desalination.,* **2011 ,** 280(1), 1–13.

[35] Lua AC; Yang T; *J. Colloid Interface Sci*., **2004,** 274(2), 594–601.

[36] Nazzal J S; Kaminska W; Michalkiewicz B; Koren Z C; *Ind Crops Prod.,* **2013,** 47,153-159.

[37] Vishwanathan B; Indra P; Neel; Varadarajan TK; *Catal Surv Asia*., **2011,** 13, 1203-1212.

[38] Yuana X; Yuana D; Zenga F; Zoua W; Tzorbatzogloub F; Tsiakarasb P; Wang Y; *Applied Catalysis B: Environmental.,* **2013 ,**129 ,367– 374.

[39] C Saka; *J.Analytical and Appl pyrolysis.,* **2012,** 95,21-24.

[40] S Jain; R V Jayaram; *Desalination.,* **2010,** 250 (3), 921–927.